arXiv:1402.4622v1 [cond-mat.stat-mech] 19 Feb 2014

Fourth virial coefficient of additive hard-sphere mixtures in the Percus–Yevick and hypernetted-chain approximations

Elena Beltrán-Heredia[1] and Andrés Santos[1, a)]
Departamento de Física, Universidad de Extremadura, Badajoz, E-06071, Spain

(Dated: 20 February 2014)

The fourth virial coefficient of additive hard-sphere mixtures, as predicted by the Percus–Yevick (PY) and hypernetted-chain (HNC) theories, is derived via the compressibility, virial, and chemical-potential routes, the outcomes being compared with exact results. Except in the case of the HNC compressibility route, the other five expressions exhibit a common structure involving the first three moments of the size distribution. In both theories the chemical-potential route is slightly better than the virial one and the best behavior is generally presented by the compressibility route. Moreover, the PY results with any of the three routes are more accurate than any of the HNC results.

I. INTRODUCTION

As is well established, the hard-sphere (HS) model plays a paradigmatic role in statistical physics, both in and out of equilibrium.[1–5] The importance of HS systems in equilibrium liquid state theory is incremented by the existence of exact solutions of the Percus–Yevick (PY) integral equation theory[2,6] both for pure[7–9] and multicomponent[10] HS fluids. In contrast, other integral equations, like the hypernetted-chain (HNC) one,[11–13] need to be solved numerically, even for HS systems.

A consequence of dealing with solutions of approximate integral equations (like PY and HNC) is that a common pair correlation function, when plugged into the so-called thermodynamic routes, gives rise to different equations of state.[2,14] This inconsistency problem is aggravated in the case of HS mixtures since the corresponding pressure depends not only on density but also on the size distribution.

The exact equation of state of HS mono- or polydisperse fluids is not analytically known, and so one has to rely on computer simulation results to assess the merits and drawbacks of approximate theories. An exception is provided by the low-density regime, in which case the equation of state can be well represented by the first few virial coefficients. The first four coefficients of pure HS fluids are analytically known[15,16] and accurate numerical evaluations of the fifth to twelfth coefficients are available.[17–21] Much less information is available for HS mixtures, the results being usually restricted to the binary case. While the second and third virial coefficients are exactly known for additive and nonadditive mixtures with any number of components,[22–26] the fourth to eighth coefficients have been numerically computed for binary mixtures at a number of size ratios and/or nonadditivities.[27–35] Recently, analytical expressions for all but one of the partial contributions to the fourth virial coefficient B_4 of additive binary mixtures have been derived[36,37] and a very accurate semi-empirical equation for the last contribution has been constructed.[36]

The aim of this paper is to evaluate B_4 (for additive HS mixtures) predicted by the PY and HNC approximations via different thermodynamic routes, and to compare them with the exact (analytical and semi-empirical) results. The two conventional routes in the case of HS systems are the compressibility and virial ones.[1,2] While B_4 from the PY theory follows from the corresponding known equations of state[10,38] in a straightforward way, we are not aware of a previous derivation of B_4 for polydisperse HS systems in the HNC theory via the virial and compressibility routes. To those conventional routes, we add the results derived from the chemical-potential route,[39–41] usually not considered in the literature. As will be shown, the PY results with any of the three routes are more accurate than any of the HNC results. Moreover, within a given theory (PY or HNC), the best behavior is due to the compressibility route, the chemical-potential results being slightly better than the virial ones.

The organization of the rest of the paper is as follows. The background material, including exact results, are presented in Sec. II. Next, the PY and HNC results are derived in Sec. III and discussed in Sec. IV. The paper is closed with some concluding remarks in Sec. V.

II. BACKGROUND

A. Thermodynamic routes

Let us consider a multicomponent HS system made of s components. The interaction between a particle of species i and a particle of species j is

$$\varphi_{ij}(r) = \begin{cases} \infty, & r < \sigma_{ij}, \\ 0, & r > \sigma_{ij}, \end{cases} \tag{2.1}$$

where σ_{ij} is the closest distance of separation for both particles. If we denote by $\sigma_i \equiv \sigma_{ii}$ and $\sigma_j \equiv \sigma_{jj}$ the diameters of particles of species i and j, respectively, we say that the HS mixture is *additive* if $\sigma_{ij} = \frac{1}{2}(\sigma_i + \sigma_j)$ for all pairs (ij). Otherwise, the mixture is said to be

a)Electronic mail: andres@unex.es; http://www.unex.es/eweb/fisteor/andres/

nonadditive. The thermodynamic state of the mixture is characterized by the total number density $\rho = N/V$ (where V and N are the volume and the total number of particles, respectively) and the mole fractions $\{x_i\}$ (with the constraint $\sum_i x_i = 1$).

In general, the knowledge of the set of radial distribution functions $g_{ij}(r;\rho)$ or, equivalently, the set of cavity functions

$$y_{ij}(r;\rho) = e^{\beta\varphi_{ij}(r)} g_{ij}(r;\rho), \tag{2.2}$$

where $\beta = 1/k_B T$ is the inverse temperature, allows one to obtain the thermodynamic properties of the fluid through the so-called thermodynamic routes.[2,14] In particular, the compressibility route reads

$$\chi_T^{-1}(\rho) \equiv \left(\frac{\partial \beta p}{\partial \rho}\right)_T = \sum_{i,j} \sqrt{x_i x_j}\left[\mathsf{I} + \hat{\mathsf{h}}(\rho)\right]^{-1}_{ij}, \tag{2.3}$$

where p is the pressure, I is the $s \times s$ unity matrix and the matrix $\hat{\mathsf{h}}$ is defined as

$$\hat{h}_{ij}(\rho) = 4\pi\rho\sqrt{x_i x_j}\int_0^\infty dr\, r^2 \left[g_{ij}(r;\rho) - 1\right]. \tag{2.4}$$

The associated compressibility factor $Z \equiv \beta p/\rho$ can be obtained as

$$Z^{(c)}(\rho) = \int_0^1 dt\, \chi_T^{-1}(\rho t). \tag{2.5}$$

The superscript in $Z^{(c)}$ means that the compressibility route has been used.

Particularized to HS mixtures, the virial (or pressure) route is

$$Z^{(v)}(\rho) = 1 + \frac{2\pi}{3}\rho \sum_{i,j} x_i x_j \sigma_{ij}^3 y_{ij}(\sigma_{ij};\rho). \tag{2.6}$$

Finally, we are here especially interested in the chemical-potential route, which has received little attention until recently.[14,39,40] In the case of HS mixtures,[40]

$$\begin{aligned}\beta\mu_i(\rho) &= \beta\mu_i^{\text{id}}(\rho) + \beta\mu_i^{\text{ex}}(\rho)\\ &= \ln\left(\rho x_i \Lambda_i^3\right) + 4\pi\rho\sum_j x_j \int_0^{\sigma_{ij}} d\sigma_{0j}\, \sigma_{0j}^2 y_{0j}(\sigma_{0j};\rho),\end{aligned} \tag{2.7}$$

where $\Lambda_i = h\sqrt{\beta/2\pi m_i}$ (h and m_i being the Planck constant and the mass of a particle of species i, respectively) is the thermal de Broglie wavelength. In Eq. (2.7), $\{y_{0j}(r)\}$ are the set of cavity functions associated with an "impurity" particle that interacts with a particle of species j via an HS potential characterized by the distance σ_{0j}. The integral over σ_{0j} describes a *charging* process from no interaction with the fluid particles ($\sigma_{0j} = 0$) to the impurity becoming a particle of species i ($\sigma_{0j} = \sigma_{ij}$). The compressibility factor derived from the chemical-potential route is[40]

$$Z^{(\mu)}(\rho) = 1 + \beta\sum_i x_i \mu_i^{\text{ex}}(\rho) - \beta\int_0^1 dt \sum_i x_i \mu_i^{\text{ex}}(\rho t). \tag{2.8}$$

In the particular case of additive mixtures, the excess term in Eq. (2.7) becomes[40]

$$\begin{aligned}\beta\mu_i^{\text{ex}}(\rho) = &-\ln(1-\eta) + 4\pi\rho\sum_j x_j\\ &\times\int_{\frac{1}{2}\sigma_j}^{\sigma_{ij}} d\sigma_{0j}\, \sigma_{0j}^2 y_{0j}(\sigma_{0j};\rho),\end{aligned} \tag{2.9}$$

where

$$\eta = \frac{\pi}{6}\rho M_3 \tag{2.10}$$

is the packing fraction,

$$M_n \equiv \sum_i x_i \sigma_i^n \tag{2.11}$$

being the nth moment of the size distribution.

B. Virial expansion

In the low-density regime, the compressibility factor can be represented as a series expansion in powers of density:

$$Z(\rho) = 1 + B_2\rho + B_3\rho^2 + B_4\rho^3 + \cdots. \tag{2.12}$$

More generally, the radial distribution functions can also be expanded as

$$g_{ij}(r;\rho) = \Theta(r-\sigma_{ij})\left[1 + y_{ij}^{(1)}(r)\rho + y_{ij}^{(2)}(r)\rho^2 + \cdots\right], \tag{2.13}$$

with

$$y_{ij}^{(1)}(r) = \sum_k x_k \mathcal{V}_{\sigma_{ik},\sigma_{kj}}(r), \tag{2.14}$$

where $\mathcal{V}_{a,b}(r)$ is the intersection volume of two spheres of radii a and b whose centers are a distance r apart. Its expression can be found in Appendix A. Equations (2.12)–(2.14) hold both for additive and nonadditive HS mixtures. Henceforth, however, we will specialize to the additive case.

Insertion of Eq. (2.13) into Eq. (2.4) yields

$$\hat{h}_{ij}(\rho) = \sqrt{x_i x_j}\rho\left[-\frac{4\pi}{3}\sigma_{ij}^3 + H_{ij}^{(1)}\rho + H_{ij}^{(2)}\rho^2 + \cdots\right], \tag{2.15}$$

with

$$\begin{aligned}H_{ij}^{(1)} =& 4\pi\int_{\sigma_{ij}}^\infty dr\, r^2 y_{ij}^{(1)}(r)\\ =& \frac{\pi^2}{36}\Big[M_6 + 6(M_5 + 2M_3\sigma_i\sigma_j)\sigma_{ij}\\ &+ 3M_4(4\sigma_{ij}^2 + \sigma_i\sigma_j)\Big],\end{aligned} \tag{2.16}$$

$$H_{ij}^{(2)} = 4\pi \int_{\sigma_{ij}}^{\infty} dr\, r^2 y_{ij}^{(2)}(r). \tag{2.17}$$

From Eqs. (2.3) and (2.5) it is easy to obtain

$$\begin{aligned} B_2 &= \frac{2\pi}{3} \sum_{i,j} x_i x_j \sigma_{ij}^3 \\ &= \frac{\pi}{6} \left(3M_1 M_2 + M_3\right), \end{aligned} \tag{2.18}$$

$$\begin{aligned} B_3 &= \frac{16\pi^2}{27} \sum_{i,j,k} x_i x_j x_k \sigma_{ik}^3 \sigma_{kj}^3 - \frac{1}{3} \sum_{i,j} x_i x_j H_{ij}^{(1)} \\ &= \left(\frac{\pi}{6}\right)^2 \left(6M_1 M_2 M_3 + 3M_2^3 + M_3^2\right), \end{aligned} \tag{2.19}$$

$$\begin{aligned} B_4^{(c)} =& \frac{16\pi^3}{27} \sum_{i,j,k,\ell} x_i x_j x_k x_\ell \sigma_{ik}^3 \sigma_{k\ell}^3 \sigma_{\ell j}^3 \\ &- \frac{2\pi}{3} \sum_{i,j,k} x_i x_j x_k \sigma_{ik}^3 H_{kj}^{(1)} - \frac{1}{4} \sum_{i,j} x_i x_j H_{ij}^{(2)}. \end{aligned} \tag{2.20}$$

The virial route is simpler. For additive mixtures, Eq. (2.14) implies

$$y_{ij}^{(1)}(\sigma_{ij}) = \frac{\pi}{6} \left(M_3 + \frac{3}{2} M_2 \frac{\sigma_i \sigma_j}{\sigma_{ij}}\right). \tag{2.21}$$

Thus, from Eq. (2.6) one recovers Eqs. (2.18) and (2.19). As for the fourth virial coefficient, Eq. (2.6) gives

$$B_4^{(v)} = \frac{2\pi}{3} \sum_{i,j} x_i x_j \sigma_{ij}^3 y_{ij}^{(2)}(\sigma_{ij}). \tag{2.22}$$

The fourth virial coefficients (2.20) and (2.22) are not expected to agree unless the exact functions $y_{ij}^{(2)}(r)$ are used.

As for the chemical-potential route, we note that $y_{0j}(\sigma_{0j};\rho)$ is given by the terms inside the square brackets in Eq. (2.13). In particular, the exact quantity $y_{0j}^{(1)}(\sigma_{0j})$ is obtained from Eq. (2.21) by the changes $\sigma_{ij} \to \sigma_{0j}$ and $\sigma_i \to 2\sigma_{0j} - \sigma_j$. As a consequence, Eq. (2.9) becomes

$$\begin{aligned} \beta\mu_i^{\text{ex}} =& \frac{\pi\rho}{6} \left(M_3 + 3M_2\sigma_i + 3M_1\sigma_i^2 + \sigma_i^3\right) + \left(\frac{\pi\rho}{6}\right)^2 \left[\frac{M_3^2}{2} + 3M_2 M_3 \sigma_i + \left(3M_1 M_3 + \frac{9M_2^2}{2}\right)\sigma_i^2 \right. \\ &\left. + \left(3M_1 M_2 + M_3\right)\sigma_i^3\right] + \left(\frac{\pi\rho}{6}\right)^3 \left[\frac{M_3^3}{3} + \frac{864}{\pi^2} \sum_j x_j \int_{\frac{1}{2}\sigma_j}^{\sigma_{ij}} d\sigma_{0j}\, \sigma_{0j}^2 y_{0j}^{(2)}(\sigma_{0j})\right] + \cdots, \end{aligned} \tag{2.23}$$

Next, application of Eq. (2.8) gives Eqs. (2.18), (2.19), and

$$B_4^{(\mu)} = \left(\frac{\pi}{6}\right)^3 \left[\frac{M_3^3}{4} + \frac{648}{\pi^2} \sum_j x_j \int_{\frac{1}{2}\sigma_j}^{\sigma_{ij}} d\sigma_{0j}\, \sigma_{0j}^2 y_{0j}^{(2)}(\sigma_{0j})\right]. \tag{2.24}$$

C. Composition-independent coefficients

The fourth virial coefficient is a fourth-degree polynomial in the mole fractions, i.e.,

$$B_4 = \sum_{i,j,k,\ell} x_i x_j x_k x_\ell B_{ijk\ell}, \tag{2.25}$$

where $B_{ijk\ell}$ are *composition-independent* coefficients that otherwise are functions of the diameters σ_i, σ_j, σ_k, and σ_ℓ. Obviously, $B_{iiii} = (\pi/6)^3 \sigma_i^9 b_4$, where b_4 is the (reduced) virial coefficient of the pure system. Thus, in the case of a binary mixture ($s = 2$) the nontrivial coefficients are B_{1112}, B_{1122}, and B_{1222}. In dimensionless form,

$$B_{1112}^*(q) \equiv \left(\frac{6}{\pi}\right)^3 \sigma_1^{-9} B_{1112}(\sigma_1, \sigma_2), \tag{2.26}$$

$$B_{1122}^*(q) \equiv \left(\frac{6}{\pi}\right)^3 \sigma_1^{-6} \sigma_2^{-3} B_{1122}(\sigma_1, \sigma_2), \tag{2.27}$$

$$B_{1222}^*(q) \equiv \left(\frac{6}{\pi}\right)^3 \sigma_1^{-3} \sigma_2^{-6} B_{1222}(\sigma_1, \sigma_2), \tag{2.28}$$

where $q \equiv \sigma_2/\sigma_1$ is the size ratio. By symmetry, $B_{1222}^*(q) = q^3 B_{1112}^*(1/q)$. Moreover, the reduced coefficients must satisfy a number of consistency conditions.[36,42–44] In particular,

$$\begin{aligned} \left.\frac{\partial B_{1112}^*(q)}{\partial q}\right|_{q=1} &= \frac{3}{2} \left.\frac{\partial B_{1122}^*(q)}{\partial q}\right|_{q=1} = 3 \left.\frac{\partial B_{1222}^*(q)}{\partial q}\right|_{q=1} \\ &= \frac{9}{4} b_4, \end{aligned} \tag{2.29}$$

$$\left.\frac{\partial B_{1112}^*(q)}{\partial q}\right|_{q=0}=\frac{9}{4},$$

$$\lim_{q\to 0} B_{1112}^*(q)=\frac{1}{4},\quad \lim_{q\to 0} B_{1122}^*(q)=2, \tag{2.30}$$

$$\lim_{q\to 0} B_{1222}^*(q)=\frac{15}{2}. \tag{2.31}$$

D. Exact results. Analytical and semi-empirical expressions for $B_{ijk\ell}^*$

The exact form of the cavity functions to second order in density, $y_{ij}^{(2)}(r)$, is not known. As a consequence, the exact composition-independent fourth virial coefficients $B_{ijk\ell}$ for any number of components is not known either. However, an interesting result refers to the case where the smallest sphere fits in the inner hole made by the other three spheres being tangent.[45] More specifically, $B_{ijk\ell}$ is analytically known if

$$\sigma_\ell \le \frac{\sigma_i\sigma_j\sigma_k}{\sigma_i\sigma_j+\sigma_i\sigma_k+\sigma_j\sigma_k+2\sqrt{\sigma_i\sigma_j\sigma_k(\sigma_i+\sigma_j+\sigma_k)}}. \tag{2.32}$$

In particular, in the case of binary mixtures ($s=2$) with $q\equiv\sigma_2/\sigma_1<2/\sqrt{3}-1\simeq 0.1547$,[45]

$$B_{1112}^*(q)=\frac{1}{4}+\frac{9q}{4}+9q^2+\frac{21q^3}{4}+\frac{27q^4}{8}+\frac{27q^5}{40}-\frac{27q^6}{5}-\frac{162q^7}{35}-\frac{81q^8}{56}-\frac{9q^9}{56}. \tag{2.33}$$

If $q>2/\sqrt{3}-1$, B_{1112}^* is given by the right-hand side of Eq. (2.33) plus the contribution[36,37]

$$\Delta B_{1112}^*(q)=\frac{1}{280\pi}\Big[\frac{Q}{12}\left(10Q^6-51Q^4+210Q^2+6976\right)-486P_1(Q^2+9)+\frac{q+1}{3}P_2\times\left(5Q^8-28Q^6\right)+129Q^4-124Q^2+11378\right)\Big], \tag{2.34}$$

where $Q\equiv\sqrt{3q^2+6q-1}$, $P_1\equiv\tan^{-1}Q$, and $P_2\equiv\tan^{-1}[Q/(q+1)]$. Because of the symmetry condition $B_{1222}^*(q)=q^3B_{1112}^*(1/q)$, the only remaining coefficient in a binary mixture is B_{1122}^*. It is made of six partial contributions, five of which are analytically known, while the sixth one needs to be numerically evaluated.[36] An accurate semi-empirical approximation of the latter partial contribution was obtained by Labík and Kolafa.[36] The combined result is

$$B_{1122}^*(q)=q^{3/2}\Big[3\left(\sqrt{q}+\frac{1}{\sqrt{q}}\right)\left(q+\frac{11}{4}+\frac{1}{q}\right)-\sqrt{2}\left(\frac{2}{u^3}+\frac{15}{4u}+\frac{9u}{5}\right)-u^3R\Big], \tag{2.35}$$

where $u\equiv\sqrt{2/(q+q^{-1})}$ and R is a rational function of u whose coefficients are listed in Table II of Ref. 36.

It is easy to check that Eqs. (2.33)–(2.35) are consistent with the one-component value

$$b_4=\frac{219\sqrt{2}-712\pi+4131\tan^{-1}\sqrt{2}}{35\pi}\simeq 18.3648 \tag{2.36}$$

and with conditions (2.29)–(2.31).

III. PERCUS–YEVICK AND HYPERNETTED-CHAIN APPROXIMATIONS

In this section the fourth virial coefficient in the PY and HNC approximations from the three routes (2.20), (2.22), and (2.24) are evaluated. To that end we need the approximate corresponding approximate expressions for $y_{ij}^{(2)}(r)$.

A. PY

The exact solution of the PY equation for additive HS mixtures is known for any density in Laplace space.[10,38] From such a solution one can get $y_{ij}^{(2,\mathrm{PY})}(r)$. Its explicit expression is given in Appendix A. In particular, the contact values are

$$y_{ij}^{(2,\mathrm{PY})}(\sigma_{ij})=\left(\frac{\pi}{6}\right)^2 M_3\left(M_3+3M_2\frac{\sigma_i\sigma_j}{\sigma_{ij}}\right). \tag{3.1}$$

Also, the integral (2.17) becomes

$$H_{ij}^{(2,\mathrm{PY})}=-\frac{\pi^3}{36}\Big[M_4M_5+4M_3M_4(\sigma_{ij}^2+\sigma_i\sigma_j)+(3M_4^2+2M_3M_5+4M_3^2\sigma_i\sigma_j)\sigma_{ij}\Big]. \tag{3.2}$$

Inserting these results unto Eqs. (2.20), (2.22), and (2.24) one obtains $B_4^{(\text{PY-}c)}$, $B_4^{(\text{PY-}v)}$, and $B_4^{(\text{PY-}\mu)}$, respectively. The three coefficients have the common structure

$$B_4=\left(\frac{\pi}{6}\right)^3 M_3\left[C_1M_1M_2M_3+C_2M_2^3+C_3M_3^2\right]. \tag{3.3}$$

The corresponding values of the PY numerical coefficients C_1, C_2, and C_3 are given in Table I. Note that only the coefficient C_2 depends on the route.

Equation (3.3) applies to any number of components s. The composition-independent virial coefficients $B_{ijk\ell}$ defined by Eq. (2.25) can be easily identified. In the particular case of a binary mixture [cf. Eqs. (2.26)–(2.28)],

$$B_{1112}^*(q)=\frac{C_1}{4}q(1+q+2q^2)+\frac{C_2}{4}q^2(3+q)+\frac{C_3}{4}(1+3q^3), \tag{3.4}$$

$$B_{1122}^*(q)=\frac{C_1}{6}(1+q)(1+q+q^2)+\frac{C_2}{2}q(1+q)+\frac{C_3}{2}(1+q^3), \tag{3.5}$$

TABLE I. Numerical coefficients C_1, C_2, and C_3 in the expression of the fourth virial coefficient [see Eq. (3.3)] according to different routes in the PY and HNC approximations. The value $b_4 = C_1 + C_2 + C_3$ is the (reduced) fourth virial coefficient in the one-component case. The three last columns indicate whether the exact consistency conditions (2.29)–(2.31) are verified or not.

Approximation	C_1	C_2	C_3	b_4	(2.29)	(2.30)	Eq. (2.31)
PY-v	9	6	1	16	Yes	Yes	No
PY-μ	9	$\frac{27}{4}$	1	$\frac{57}{4}$	Yes	Yes	No
PY-c	9	9	1	19	Yes	Yes	Yes
HNC-v	$\frac{27}{2}$	$\frac{27}{2}$	$\frac{3}{2}$	$\frac{57}{2}$	Yes	No	No
HNC-μ	$\frac{27}{2}$	$\frac{27}{2}$	$\frac{11}{8}$	$\frac{227}{8}$	Yes	No	No
HNC-c	–	–	–	$\frac{5623}{420}$	Yes	No	No

$$B_{1222}^*(q) = \frac{C_1}{4}(2+q+q^2)+\frac{C_2}{4}(1+3q)+\frac{C_3}{4}(3+q^3). \quad (3.6)$$

From Eqs. (3.4)–(3.6) we can see that conditions (2.29) are automatically satisfied regardless of the numerical values of the coefficients C_1, C_2, and C_3. On the other hand, the three conditions in (2.30) are fulfilled only if $C_1 = 9$, $C_3 = 1$ and $C_1 + 3C_3 = 12$, respectively. Thus, the three PY routes turn out to be consistent with Eqs. (2.29) and (2.30). As for Eq. (2.31), it requires $2C_1 + C_2 + 3C_3 = 30$, this condition being satisfied by the compressibility route only.

B. HNC

In the case of the HNC approximation one has[2,14]

$$y_{ij}^{(2,\text{HNC})}(r) = y_{ij}^{(2,\text{PY})}(r) + \frac{1}{2}\left[y_{ij}^{(1)}(r)\right]^2. \quad (3.7)$$

Consequently,

$$y_{ij}^{(2,\text{HNC})}(\sigma_{ij}) = \left(\frac{\pi}{6}\right)^2\left[\frac{3}{2}M_3\left(M_3 + 3M_2\frac{\sigma_i\sigma_j}{\sigma_{ij}}\right) + \frac{9}{8}M_2^2\left(\frac{\sigma_i\sigma_j}{\sigma_{ij}}\right)^2\right], \quad (3.8)$$

$$H_{ij}^{(2,\text{HNC})} = H_{ij}^{(2,\text{PY})} + 2\pi\int_{\sigma_{ij}}^{\infty} dr\,[ry_{ij}^{(1)}(r)]^2. \quad (3.9)$$

Let us start by considering the virial and chemical-potential routes. By plugging Eq. (3.8) into Eqs. (2.22) and (2.24) one finds again results of the form (3.3), except that the values of the coefficients C_1–C_3 differ from the PY ones. Those values are given in Table I. We observe that the exact relationship $B_4^{(\text{HNC-}v)} = \frac{3}{2}B_4^{(\text{PY-}c)}$, valid for any interaction and any dimensionality,[46] is indeed verified. It is also interesting to remark that $B_4^{(\text{HNC-}v)} \simeq B_4^{(\text{HNC-}\mu)}$ since both quantities differ only in the coefficient C_3, which is $\frac{12}{11} \simeq 1.09$ times larger in the virial route than in the chemical-potential route. As a consequence, $b_4^{(\text{HNC-}v)}/b_4^{(\text{HNC-}\mu)} = \frac{228}{227} \simeq 1.004$ in the pure fluid. In the case of a binary mixture, the composition independent coefficients $B_{ijk\ell}^{*(\text{HNC-}v)}$ and $B_{ijk\ell}^{*(\text{HNC-}\mu)}$ are given by Eqs. (3.4)–(3.6) with the corresponding values of C_1–C_3. Now only the consistency conditions (2.29) are satisfied.

Regarding the compressibility route, one has

$$B_4^{(\text{HNC-}c)} = B_4^{(\text{PY-}c)} - \frac{\pi}{2}\sum_{i,j}x_ix_j\int_{\sigma_{ij}}^{\infty} dr\,[ry_{ij}^{(1)}(r)]^2. \quad (3.10)$$

As discussed in Appendix B, the second term on the right-hand side of Eq. (3.10) prevents $B_4^{(\text{HNC-}c)}$ from accommodating to the simple structure of Eq. (3.3). First, moments of order higher than M_3 are involved. Second, there exist terms that cannot be accounted for by moments since those extra terms depend on the size order of the species and thus they are not invariant under a relabeling of species. After some algebra, the obtained result is

$$\left(\frac{6}{\pi}\right)^3 B_4^{(\text{HNC-}c)} = \left(\frac{6}{\pi}\right)^3 B_4^{(\text{PY-}c)} + M_1\left(\frac{27}{40}M_1^2M_6 + \frac{63}{40}M_1M_2M_5 - \frac{9}{8}M_1M_3M_4 - \frac{9}{280}M_1M_7 - \frac{9}{8}M_2^2M_4 - \frac{3}{2}M_2M_3^2 + \frac{3}{20}M_2M_6 - \frac{3}{4}M_3M_5 - \frac{3}{28}M_8\right) - M_2\left(\frac{9}{4}M_2^2M_3 + \frac{9}{40}M_2M_5 + \frac{3}{4}M_3M_4 + \frac{3}{280}M_7\right) - \frac{1}{8}M_3M_6 - \frac{1}{84}M_9 - \mathcal{B}, \quad (3.11)$$

where, in the particular case of a binary mixture (assuming $q \equiv \sigma_2/\sigma_1 \leq 1$), the expression for the extra term $\mathcal{B}$

is

$$\mathcal{B} = \sigma_1^9 x_1 x_2 \frac{(1-q)^5}{105}\Big\{\frac{1-q}{4}\left[x_1^2(1039+393q+75q^2+5q^3)\right.$$
$$\left.-x_2^2(1039q^3+393q^2+75q+5)\right]$$
$$-\frac{179M_1M_3+174M_2^2+25M_4}{\sigma_1^4}\Big\}. \tag{3.12}$$

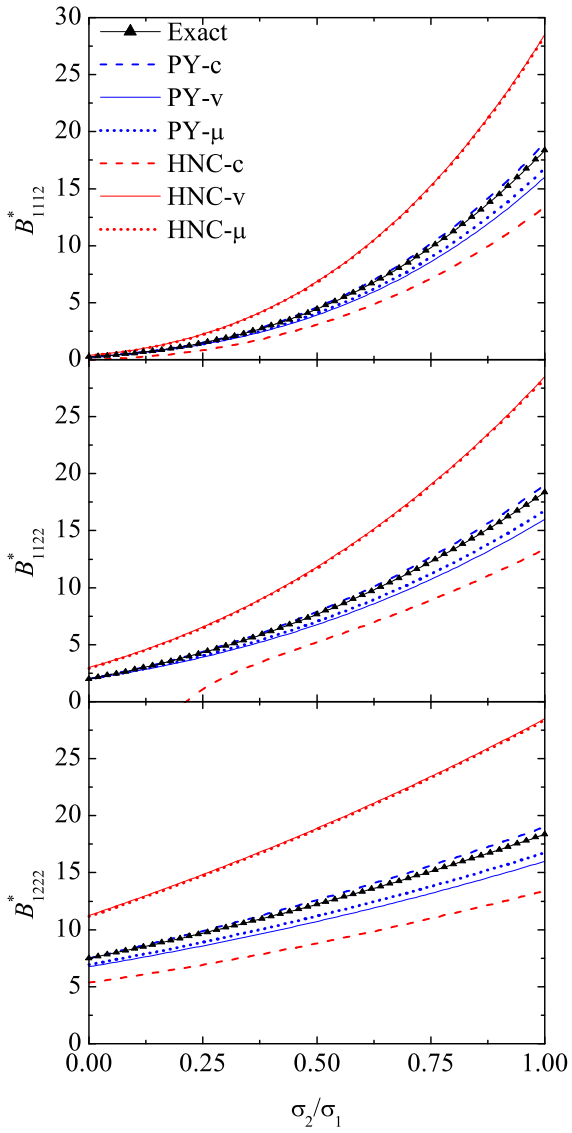

FIG. 1. Comparison between exact and approximate composition-independent virial coefficients B^*_{1112}, B^*_{1122}, and B^*_{1222}.

In the case of the HNC compressibility route for a binary mixture, Eqs. (3.11) and (3.12) yield (assuming again $q \le 1$)

$$B_{1112}^{*(\text{HNC-}c)} = -\frac{1}{1680}+\frac{621q}{560}+\frac{531q^2}{70}+\frac{45q^3}{8}-\frac{3q^4}{2}$$
$$+\frac{3q^5}{10}+\frac{7q^6}{20}-\frac{3q^7}{140}-\frac{3q^8}{56}-\frac{q^9}{168}, \tag{3.13}$$

$$B_{1122}^{*(\text{HNC-}c)} = -\frac{17q^{-3}}{2520}-\frac{17q^{-2}}{280}-\frac{17q^{-1}}{70}+\frac{8}{5}+\frac{261q}{40}$$
$$+\frac{141q^2}{40}+\frac{5q^3}{3}+\frac{7q^4}{10}-\frac{13q^5}{56}-\frac{31q^6}{360}, \tag{3.14}$$

$$B_{1222}^{*(\text{HNC-}c)} = \frac{43}{8}+\frac{759q}{140}+\frac{1767q^2}{560}-\frac{947q^3}{1680}. \tag{3.15}$$

As happened with the virial and chemical-potential routes, only Eq. (2.29) is satisfied by $B_{ijk\ell}^{*(\text{HNC-}c)}$.

IV. DISCUSSION

Figure 1 compares the PY and HNC predictions via the virial, compressibility, and chemical-potential routes with the exact results for the composition-independent fourth virial coefficients. Several comments are in order in view of of Fig. 1 and of the results derived in the preceding section:

i As anticipated from the coefficients in Table I, we observe that $B_{ijk\ell}^{*(\text{HNC-}v)}$ and $B_{ijk\ell}^{*(\text{HNC-}\mu)}$ are practically indistinguishable.

ii While in the PY approximation the virial and chemical-potential routes underestimate the virial coefficients and the compressibility route overestimates them, the opposite behavior is observed in the case of the HNC approximation.

iii As mentioned above, and as a test of the results, the general property $B_{ijk\ell}^{*(\text{HNC-}v)} = \frac{3}{2}B_{ijk\ell}^{*(\text{PY-}c)}$ is satisfied.

iv The three PY predictions are more accurate than any of the HNC predictions.

v In both approximations, the chemical-potential route is slightly better than the virial one.

vi In both approximations, the compressibility route is the most accurate one, except in the case of the HNC cofficient B^*_{1122} for $\sigma_2/\sigma_1 \lesssim 0.315$.

vii The coefficients $B_{1112}^{*(\text{HNC-}c)}$ and $B_{1122}^{*(\text{HNC-}c)}$ become negative for $\sigma_2/\sigma_1 \lesssim 0.00053$ and $\sigma_2/\sigma_1 \lesssim 0.213$, respectively. Moreover, $B_{1122}^{*(\text{HNC-}c)}$ diverges to $-\infty$ in the limit $\sigma_2/\sigma_1 \to 0$.

viii Except for $B_4^{*(\text{HNC-}c)}$, the other five theoretical predictions depend on the size composition only through the first three moments and have the common structure (3.3).

V. CONCLUDING REMARKS

The results presented in this paper confirm that, even though the HNC approximation retains more diagrams than the PY one,[2,14] it is certainly less reliable than the latter when applied to HS systems. It is well known that the energy and virial routes are fully equivalent for any system in the HNC theory.[1,13] Our results show that, in addition, the chemical-potential and virial routes are practically identical, at least at the level of the fourth virial coefficient for polydisperse HS fluids. Thus, we are in the presence of a neat example showing that a high degree of internal consistency does not necessarily correlate with accuracy.

It is also interesting to note that in both theories the compressibility route (which needs the whole spatial dependence of the pair correlation functions) is generally more efficient than the virial and chemical-potential routes (which only need the contact values) in concealing the deficiencies associated with the approximate nature of the theory. On the other hand, this feature seems to be restricted to highly repulsive interactions since the addition of an attractive part (as in the sticky-hard-sphere model) tends to worsen the quality of the compressibility route and makes the chemical-potential route the most accurate one.[41]

To conclude, we hope that this paper can contribute to a better understanding of the merits, shortcomings, and peculiarities of the two classical integral equations when applied to such an important model as the HS multicomponent fluid.

ACKNOWLEDGMENTS

A.S. acknowledges the financial support of the Spanish Government through Grant No. FIS2010-16587 and the Junta de Extremadura (Spain) through Grant No. GR10158 (partially financed by FEDER funds).

Appendix A: Supplementary equations

In this Appendix we include some equations that, for conciseness, are omitted in the main text.

First, the formula for the overlap volume $\mathcal{V}_{a,b}(r)$ is

$$\mathcal{V}_{a,b}(r)=\begin{cases}\frac{4\pi}{3}\min(a^3,b^3), & 0<r<|a-b|,\\ W_{a,b}(r), & |a-b|<r<a+b,\\ 0, & r>a+b,\end{cases} \tag{A1}$$

with

$$W_{a,b}(r)=\frac{\pi(a+b-r)^2[r^2+2(a+b)r-3(a-b)^2]}{12r}. \tag{A2}$$

Next, the PY expression for $y_{ij}^{(2,\mathrm{PY})}(r)$ is

$$\begin{aligned}y_{ij}^{(2,\mathrm{PY})}(r)=&\frac{\pi}{3}M_3y_{ij}^{(1)}(r)+\left(\frac{\pi}{6}\right)^2\frac{1}{r}\Big[\sum_k x_k\Theta(\sigma_k+\sigma_{ij}-r)(\sigma_k+\sigma_{ij}-r)^2F_{ij;k}(r)\\&+\sum_{k,\ell}x_kx_\ell\Theta(\sigma_k+\sigma_\ell+\sigma_{ij}-r)(\sigma_k+\sigma_\ell+\sigma_{ij}-r)^4F_{ij;k\ell}(r)\Big],\end{aligned} \tag{A3}$$

where

$$\begin{aligned}F_{ij;k}(r)=&\frac{(\sigma_k+\sigma_{ij}-r)^2}{70}\Big[4(\sigma_{ij}-r)^2(6\sigma_{ij}+r)+21(\sigma_i\sigma_j-M_2)(3\sigma_k+2r-2\sigma_{ij})+\sigma_k\sigma_{ij}\\&\times(9\sigma_k+38r-54\sigma_{ij})-2\sigma_k(\sigma_k+r)(9\sigma_k-8r)\Big]+M_1\frac{3(\sigma_k+\sigma_{ij}-r)}{10}\\&\times\Big\{5\sigma_i\sigma_j(3\sigma_k+r-\sigma_{ij})+2\sigma_{ij}(r-\sigma_{ij})\,(8\sigma_k+r-\sigma_{ij})+\sigma_k[2(r-\sigma_{ij})^2\\&-\sigma_k(3\sigma_k-\sigma_{ij}-r)]\Big\}+M_2\Big\{9\sigma_i\sigma_j\sigma_k+\frac{3}{2}\sigma_{ij}\left[\sigma_k^2+6\sigma_k(r-\sigma_{ij})-(r-\sigma_{ij})^2\right]\Big\},\end{aligned} \tag{A4}$$

$$\begin{aligned}F_{ij;k\ell}(r)=&-\frac{6}{35}(\sigma_k+\sigma_\ell+\sigma_{ij}-r)^3-\frac{r}{5}(\sigma_k+\sigma_\ell+\sigma_{ij}-r)^2+\frac{6}{5}(\sigma_k+\sigma_\ell+\sigma_{ij}-r)\\&\times(\sigma_{ik}\sigma_{\ell j}+\sigma_{ik}\sigma_{k\ell}+\sigma_{k\ell}\sigma_{\ell j})-6\sigma_{ik}\sigma_{k\ell}\sigma_{\ell j}.\end{aligned} \tag{A5}$$

Appendix B: The compressibility route in the HNC approximation

In the application of the compressibility route in the HNC approximation [see Eq. (3.10)] one has to deal with the term

$$\sum_{i,j}x_ix_j\int_{\sigma_{ij}}^\infty dr\,[ry_{ij}^{(1)}(r)]^2. \tag{B1}$$

According to Eqs. (2.14) and (A1), the mathematical structure of $[y_{ij}^{(1)}(r)]^2$ for $r > |\sigma_i - \sigma_j|$ is

$$
\begin{aligned}
[y_{ij}^{(1)}(r)]^2 =& \sum_{k,\ell} x_k x_\ell \Theta(\sigma_{ij} + \sigma_k - r)\Theta(\sigma_{ij} + \sigma_\ell - r) \\
& \times W_{\sigma_{ik},\sigma_{kj}}(r) W_{\sigma_{i\ell},\sigma_{\ell j}}(r) \\
=& \sum_{k,\ell} x_k x_\ell \Theta(\sigma_{ij} + \sigma_k - r) W_{\sigma_{ik},\sigma_{kj}}(r) W_{\sigma_{i\ell},\sigma_{\ell j}}(r) \\
& - \sum_{k,\ell} x_k x_\ell \Theta(\sigma_{ij} + \sigma_k - r)\Theta(r - \sigma_{ij} - \sigma_\ell) \\
& \times W_{\sigma_{ik},\sigma_{kj}}(r) W_{\sigma_{i\ell},\sigma_{\ell j}}(r), \qquad \text{(B2)}
\end{aligned}
$$

where in the second step we have used the property $\Theta(x) = 1 - \Theta(-x)$. Now, without loss of generality, we assume that $\sigma_1 \geq \sigma_2 \geq \cdots \geq \sigma_s$. In that case, $\Theta(\sigma_{ij} + \sigma_k - r)\Theta(r - \sigma_{ij} - \sigma_\ell) = 0$ if $k \geq \ell$. Therefore,

$$
\begin{aligned}
[y_{ij}^{(1)}(r)]^2 =& \sum_{k,\ell} x_k x_\ell \Theta(\sigma_{ij} + \sigma_k - r) W_{\sigma_{ik},\sigma_{kj}}(r) W_{\sigma_{i\ell},\sigma_{\ell j}}(r) \\
& - \sum_{k<\ell} x_k x_\ell \Theta(\sigma_{ij} + \sigma_k - r)\Theta(r - \sigma_{ij} - \sigma_\ell) \\
& \times W_{\sigma_{ik},\sigma_{kj}}(r) W_{\sigma_{i\ell},\sigma_{\ell j}}(r). \qquad \text{(B3)}
\end{aligned}
$$

When inserted into Eq. (B1), the first term on the right-hand side of Eq. (B3) gives rise to the contribution in Eq. (3.11) expressed in terms of the first nine moments of the size distribution. On the other hand, the contribution associated with the second term on the right-hand side of Eq. (B3) is not invariant under a relabeling of indices because of the constraint $k < \ell$. Such a contribution is given by Eq. (3.12) in the particular case of a binary mixture.

[1] J. A. Barker and D. Henderson, Rev. Mod. Phys. **48**, 587 (1976).
[2] J.-P. Hansen and I. R. McDonald, *Theory of Simple Liquids* (Academic, London, 2006).
[3] C. N. Likos, Phys. Rep. **348**, 267 (2001).
[4] A. Mulero, ed., *Theory and Simulation of Hard-Sphere Fluids and Related Systems* (Springer-Verlag, Berlin, 2008), vol. 753 of *Lectures Notes in Physics*.
[5] J. R. Solana, *Perturbation Theories for the Thermodynamic Properties of Fluids and Solids* (CRC Press, Boca Raton, 2013).
[6] J. K. Percus and G. J. Yevick, Phys. Rev. **110**, 1 (1958).
[7] M. S. Wertheim, Phys. Rev. Lett. **10**, 321 (1963).
[8] E. Thiele, J. Chem. Phys. **39**, 474 (1963).
[9] M. S. Wertheim, J. Math. Phys. **5**, 643 (1964).
[10] J. L. Lebowitz, Phys. Rev. **133**, A895 (1964).
[11] T. Morita, Prog. Theor. Phys. **20**, 920 (1958).
[12] J. M. J. van Leeuwen, J. Groeneveld, and J. de Boer, Physica **25**, 792 (1959).
[13] T. Morita, Prog. Theor. Phys. **23**, 829 (1960).
[14] A. Santos, *Playing with Marbles: Structural and Thermodynamic Properties of Hard-Sphere Systems*, arXiv:1310.5578 (2013).
[15] N. Clisby and B. McCoy, J. Stat. Phys. **114**, 1361 (2004).
[16] I. Lyberg, J. Stat. Phys. **119**, 747 (2005).
[17] N. Clisby and B. M. McCoy, J. Stat. Phys. **114**, 1343 (2004).
[18] S. Labík, J. Kolafa, and A. Malijevský, Phys. Rev. E **71**, 021105 (2005).
[19] N. Clisby and B. M. McCoy, Pramana **64**, 775 (2005).
[20] N. Clisby and B. M. McCoy, J. Stat. Phys. **122**, 15 (2006).
[21] R. J. Wheatley, Phys. Rev. Lett. **110**, 200601 (2013).
[22] T. Kihara, Rev. Mod. Phys. **27**, 412 (1955).
[23] T. Kihara and K. Miyoshi, J. Stat. Phys. **13**, 337 (1975).
[24] E. Z. Hamad, J. Chem. Phys. **105**, 3222 (1996).
[25] E. Z. Hamad, J. Chem. Phys. **105**, 3229 (1996).
[26] M. Al-Naafa, J. B. El-Yakubu, and E. Z. Hamad, Fluid Phase Equil. **154**, 33 (1999).
[27] F. Saija, G. Fiumara, and P. V. Giaquinta, Mol. Phys. **87**, 991 (1996).
[28] F. Saija, G. Fiumara, and P. V. Giaquinta, Mol. Phys. **92**, 1089 (1997).
[29] E. Enciso, N. G. Almarza, D. S. Calzas, and M. A. González, Mol. Phys. **92**, 173 (1997).
[30] E. Enciso, N. G. Almarza, M. A. González, and F. J. Bermejo, Phys. Rev. E **57**, 4486 (1998).
[31] R. J. Wheatley, F. Saija, and P. V. Giaquinta, Mol. Phys. **94**, 877 (1998).
[32] F. Saija, G. Fiumara, and P. V. Giaquinta, J. Chem. Phys. **108**, 9098 (1998).
[33] A. Y. Vlasov and A. J. Masters, Fluid Phase Equil. **212**, 183 (2003).
[34] G. Pellicane, C. Caccamo, P. V. Giaquinta, and F. Saija, J. Phys. Chem. B **111**, 4503 (2007).
[35] M. López de Haro, A. Malijevský, and S. Labík, Coll. Czech. Chem. Commun. **75**, 359 (2010).
[36] S. Labík and J. Kolafa, Phys. Rev. E **80**, 051122 (2009).
[37] I. Urrutia, Phy. Rev. E **84**, 062101 (2011).
[38] S. B. Yuste, A. Santos, and M. López de Haro, J. Chem. Phys. **108**, 3683 (1998).
[39] A. Santos, Phys. Rev. Lett. **109**, 120601 (2012).
[40] A. Santos and R. D. Rohrmann, Phys. Rev. E **87**, 052138 (2013).
[41] R. D. Rohrmann and A. Santos, *Equation of state of sticky-hard-sphere fluids in the chemical-potential route*, arXiv:1401.3549 (2014).
[42] R. J. Wheatley, Mol. Phys. **93**, 965 (1998).
[43] R. J. Wheatley, J. Chem. Phys. **111**, 5455 (1999).
[44] C. Barrio and J. R. Solana, in *Theory and Simulation of Hard-Sphere Fluids and Related Systems*, edited by A. Mulero (Springer-Verlag, Berlin, 2008), vol. 753 of *Lectures Notes in Physics*, pp. 133–182.
[45] R. Blaak, Mol. Phys. **95**, 695 (1998).
[46] A. Santos and G. Manzano, J. Chem. Phys. **132**, 144508 (2010).